International Journal of Radiology and Diagnostic Imaging

E-ISSN: 2664-4444
P-ISSN: 2664-4436
www.radiologypaper.com
IJRDI 2024; 7(1): 01-07
Received: 03-10-2023
Accepted: 12-11-2023

Dr. Noran Mohammed Shams El Dine
Department of Radio-diagnosis and Medical Imaging, Faculty of medicine Tanta University, Egypt

Dr. Mohammed Mahmoud Dawoud
Department of Radio-diagnosis and Medical Imaging, Faculty of medicine, Tanta University, Egypt

Dr. Noha Mohammed Abd El-mabod
Department of Radio-diagnosis and Medical Imaging, Faculty of medicine, Tanta University, Egypt

Dr. Basma Samir El- Deeb
Department of Radio-diagnosis and Medical Imaging, Faculty of medicine, Tanta University, Egypt

Corresponding Author:
Dr. Noran Mohammed Shams El Dine
Department of Radio-diagnosis and Medical Imaging, Faculty of medicine Tanta University, Egypt

Functional magnetic resonance imaging (MRI) in diagnosis of pelvic endometriosis

Dr. Noran Mohammed Shams El Dine, Dr. Mohammed Mahmoud Dawoud, Dr. Noha Mohammed Abd El-mabod and Dr. Basma Samir El-Deeb

DOI: https://doi.org/10.33545/26644436.2024.v7.i1a.359

Abstract

Background: Pelvic discomfort and infertility are two potential side effects of endometriosis, a chronic multifocal gynecologic condition that mostly affects women of childbearing age. This research aimed to characterise the various pelvic endometriosis manifestations as shown on functional MRI.

Methods: Female patients aged 18 and up who were referred from the gynaecology and obstetrics department to the Radiodiagnosis and medical imagining department at Tanta University Hospitals for evaluation of a clinical suspicion of pelvic endometriosis or during an abdominal or trans-vaginal ultrasound examination were included in this cross-sectional prospective study.

Results: By laparoscopy, 27 patients tested positive. Twenty-six positive instances were found using MRI with supplemental DWI, SWI, and DCE. There was one tubal case, two CS cases, four deep infiltrating cases, ten adenomyosis cases, and nine ovarian endometrioma cases among the positive cases. Improved sensitivity of 96.3%, 100% PPV, and 93.3% accuracy were all achieved by combining DWI, SWI, and DCE MRI for the diagnosis of endometriosis.

Conclusions: Since DWI and SWI can identify the hemorrhagic nature of endometriotic lesions, they may be used in lieu of invasive laparoscopy to make a diagnosis of endometriosis, which greatly improves the diagnostic accuracy of MRI.

Keywords: Magnetic resonance imaging, pelvic, endometriosis

Introduction

Pelvic discomfort and infertility are two potential side effects of endometriosis, a chronic multifocal gynecologic condition that mostly affects women of childbearing age. Endometriosis has a complicated pathophysiology that has not been fully understood. Its origin is uncertain. The condition manifests itself in the development of endometrial glands and stroma outside of the uterus, where they do not belong [1].

Endometriosis has a frequency of between 5 and 20 percent and may present with or without symptoms. Hormonal stimulation of the ectopic endometrium causes varying degrees of cyclic bleeding, leading to symptoms and imaging characteristics that are diagnostic of endometriosis [2].

Although ultrasound (US) is often used as a preliminary diagnostic tool for endometriotic lesions, magnetic resonance imaging (MRI) has many benefits over US, including improved picture reproducibility and a wider field of view that enables the identification of illness beyond the pelvis [3]. Despite the widespread acceptance of laparoscopy as the gold standard for diagnosis, magnetic resonance imaging (MRI) is increasingly being acknowledged as an important part of both the initial assessment and the subsequent stages of patient care [4]. Endometriosis is characterised by ectopic endometrial bleeding that causes cystic bleeding and the subsequent accumulation of concentrated hemosiderin [4]. The relatively new MRI technology of susceptibility-weighted MRI provides very high sensitivity to blood products and enhances sensitivity to susceptibility effects. Signal voids owing to hemosiderin deposition along the cyst wall were clearly seen, confirming that endometrioma is characterised by the deposition of hemosiderin-laden macrophages in the cyst wall as a result of repetitive bleeding [5]. Differentiating between adenomyosis and fibroids may be greatly aided by the use of diffusion weighted images (DWI) and apparent diffusion coefficient (ADC) values.

The ADC values of fibroids and adenomyosis were found to be significantly different from those of the myometrium. All of this points to a cellular makeup that is unique to these tissues [6]. Enhancing endometriotic mural nodules have a time-signal intensity curve characterised by an early peak enhancement and a sustained plateau, making dynamic MRI a promising tool for detecting the potential malignant transformation of these lesions. Lesion time-signal intensity curves may suggest endometriosis because they resemble those of the uterine endometrium [7].

This research aimed to characterize the various pelvic endometriosis manifestations as shown on functional MRI.

Patients and Methods

Female patients aged 18 and up who were referred from the gynaecology and obstetrics department to the Radiodiagnosis and medical imagining department at Tanta University Hospitals for evaluation of a clinical suspicion of pelvic endometriosis or during an abdominal or trans-vaginal ultrasound examination were included in this cross-sectional prospective study. Tanta University's Medical School's Research Ethical Committee gave its stamp of approval to the research. Between April 2020 and April 2022, this research was conducted. After thoroughly explaining the advantages, we received written informed consents from all patients. The patient will be reassured and educated about the advantages of the MRI test if any potential dangers, such as claustrophobia, arise throughout the course of the investigation.

Inclusion criteria were all patients who satisfied the inclusion criteria-females of childbearing age who were suspected clinically or by ultrasonography to have pelvic endometriosis were included.

Exclusion criteria were Patients with clipped aneurysms, cochlear implants, or cardiac pacemakers; patients with severe allergies to intravenous contrast agents; patients with impaired renal or hepatic function; and patients who decline evaluation owing to claustrophobia.

All patients were subjected to the following

- Complete medical history and physical examination:
- The clinical evaluation includes a complete physical examination as well as an assessment of the abdomen and pelvis.
- Complete blood count (CBC), random blood sugar, liver and kidney function tests, and other routine laboratory investigations are performed on all patients.

Ultrasonography (both abdominal and transvaginal) and magnetic resonance imaging (MRI) were performed on all patients.

Pelvic MRI study

Patient preparation: In order to decrease intestinal peristalsis during MR imaging, an antispasmodic medication (10 mg of visceralgine) was administered intravenously just before to the procedure. Before being examined, the patient took off all of her jewellery and emptied her bladder (to prevent her irritability during examination). The patients were reassured by being told what to expect throughout the test and why it was important for them to stay still for the whole duration.

MR imaging protocol

Most scans were performed on a GE Signa explorer 1.5 Tesla MRI unit, while the remainder were performed on a SIMENSE machine1.5 Tesla MRI unit.

Position of the patient

Each patient was examined while lying supine on a comfortable examination table.

The body coil is placed over the pelvis, and the spine coil is placed under the patient's back (From iliac crest down to mid-thigh). Conventional MRI was performed first on patients, then DW-MRI, then SWI, and lastly DCE-MRI was added in situations where it was suspected. Time spent on the test varied between 15 and 45 minutes.

Protocol for MRI Pelvis

Pre contrast Sequences

Standard MRI sequences

MRI consideration: FOV: (FH=300 mm, RL= 300mm, AP=150 mm).

Slice thickness: 5 mm, 8 mm.

Slice number: 25

T2 WI (sagittal, coronal, axial): TR: 4000-7000 ms, TE: 110-120 ms.

T1 WI (sagittal, axial, FAT, SAT): TR: 450-650 ms, TE: 10-16 ms.

Diffusion weighted imaging (DW-MRI)

Sagittal focused DWI-MRI was obtained in the sagittal plane to identify uterine and cervical masses, whereas axial focused DWI-MRI was collected in the axial plane before the injection of contrast medium. In an axial technique, we collected several b values of (400), (800), and (1000).

Susceptibility weighted MRI: Axial eSWAN sequence was done

Protocol for SWI Pelvis (applied in axial sequences)

(Scan Plane: Oblique FOV: (47mm) - Slice thickness: 3.6 mm)

(Slice Spacing: 1 mm, Number of slices: 25)

(TR: 79.2 ms, TE: 49.8 ms)

(Matrix: 228x192, Flip angel: 20◦)

To enhance the visibility of susceptibility-induced signal voids, automatically post-processing filtered phase was applied.

Dynamic contrast-enhanced MRI

After manually injecting gadolinium at a dosage of 0.1 mmol/kg of body weight (Maximum, 20 mL), post-contrast gradient pictures were acquired, and then the tube was flushed with 20 mL of normal saline. In around 5 stages, we spent about 120 seconds acquiring consecutive images. Finally, delayed T1-weighted gradient-echo pictures of the axial, sagittal, and coronal planes were obtained.

MR imaging analysis

The uterus, cervix, fallopian tubes, and ovaries were all studied using MR imaging.

How the mass appears on MRI; cystic, solid, or a combination of the two. The extent of the injury. The strength of the mass signal across all pulse patterns. Endometrial thickness. Homogeneous, heterogeneous, mild, moderate, or strong enhancement of the uterus and cervical region in DCE MRI scans. T2-weighted pictures, DCE images, and DWI, along with a slew of gynaecological and cervical/vaginal/parametro and upward/downward flexion/ extension images.

Interpretation of DWI

Qualitative analysis: If the masses have low signal intensity on diffusion images but high signal at ADC or high signal at both diffusion and ADC in the corresponding ADC maps (facilitated), or if the masses have high signal intensity on diffusion images but lower signal in the corresponding ADC maps, or if the masses have heterogeneous signal at both diffusion and ADC, we make a comment on this (restricted). Intense signals in both DWI and ADC were seen for certain masses (Shine through effect).

Quantitative analysis

If the masses have low signal intensity on diffusion images but high signal at ADC or high in both diffusion and ADC in the corresponding ADC maps (Facilitated), or if the masses have high signal intensity on diffusion images but lower signal in the corresponding ADC maps, or if the masses have heterogeneous signal at both diffusion and ADC, we make a comment on this (Restricted). Both DWI and ADC exhibited quite intense signal at several masses (Shine through effect).

Interpretation of DCE-MRI

Consensus-based, real-time data analysis using a desktop computer. At 120 seconds after gadolinium injection, the complete mass is acquired over all five phases of the dynamic run. To use colour map, a manual area of interest (ROI) is created across the lesion's most strongly augmenting mass, solid component, thick enhanced wall, or septations. A plot of signal intensity (SI) vs time was generated. Benign lesions showed a type I time intensity curve (a steady upward trend), borderline lesions showed a type II (a plateau trend), and malignant lesions showed a type III (a sharp upward trend followed by a quick decline).

Interpretation of SWI-MRI

At the SWI, researchers looked for susceptibility artefact around the mass lesion, which might have been caused by either calcification or the ageing of a blood product. Filter phase sequence of SWI processed automatically on the work station helped differentiate between blood product and calcification by making signal voids of blood product appear as high signal intensity and calcification remaining as signal voids.

Case (1)

Clinical presentation included right iliac fossa discomfort and vaginal bleeding in a 30-year-old female patient.

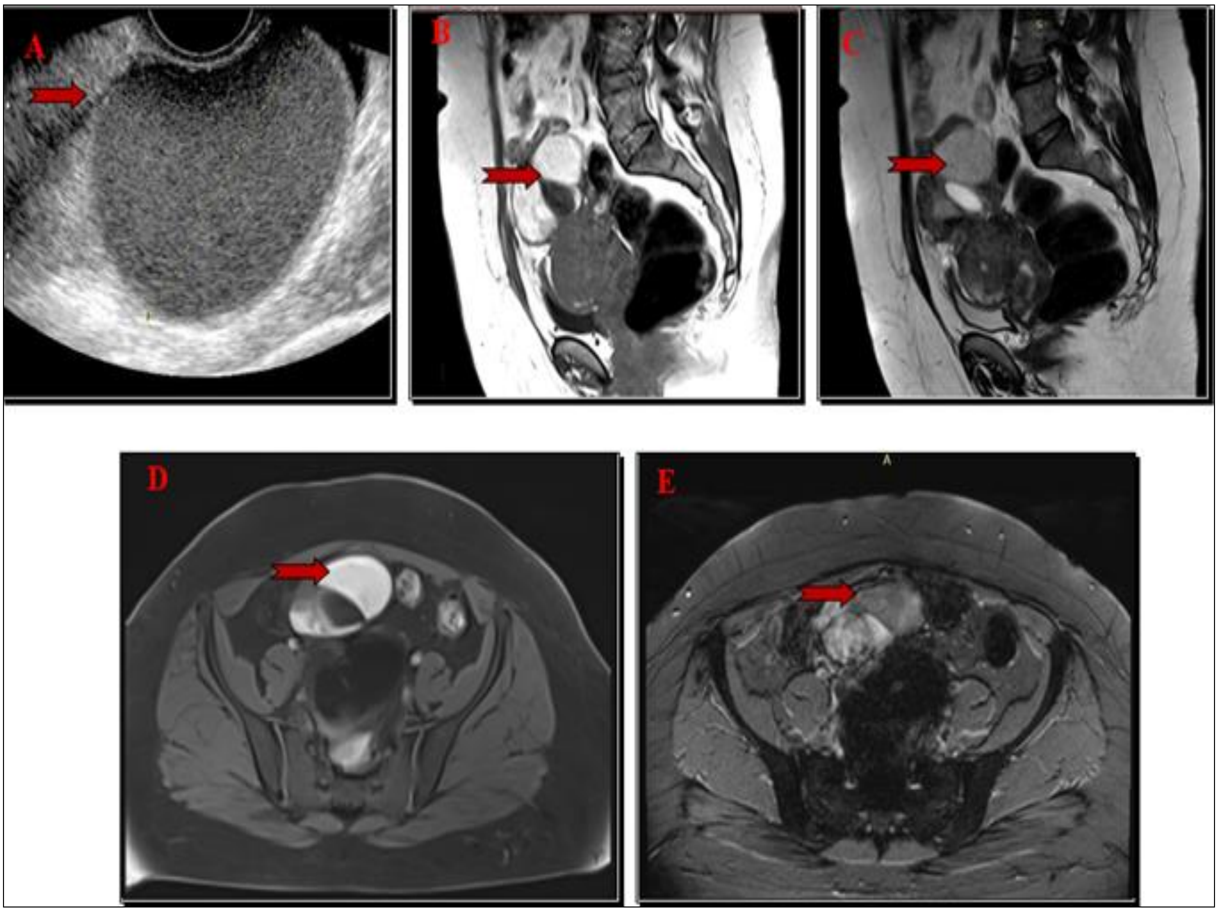

Fig 1: (A) Ultrasound showed a well-defined cystic lesion related to right adenxia with hemorrhagic internal echoes with no vascularity on colour Doppler study. (B) MRI sagittal T_1, (C) MRI sagittal T_2, (D) MRI axial T_1 FAT SAT and (E) MRI axial T_2 FAT SAT revealed: well defined right ovarian cystic lesion displayed high signal intensity in T_1 and low signal intensity in T_2 (shadding sign)

Case (2)

Persistent pelvic discomfort, dysparunea, and chronic constipation were the primary complaints of a 42-year-old female patient who came to the clinic. Previous left oophorectomy and hysterectomy patient (adenomyosis & ovarian endometrioma).

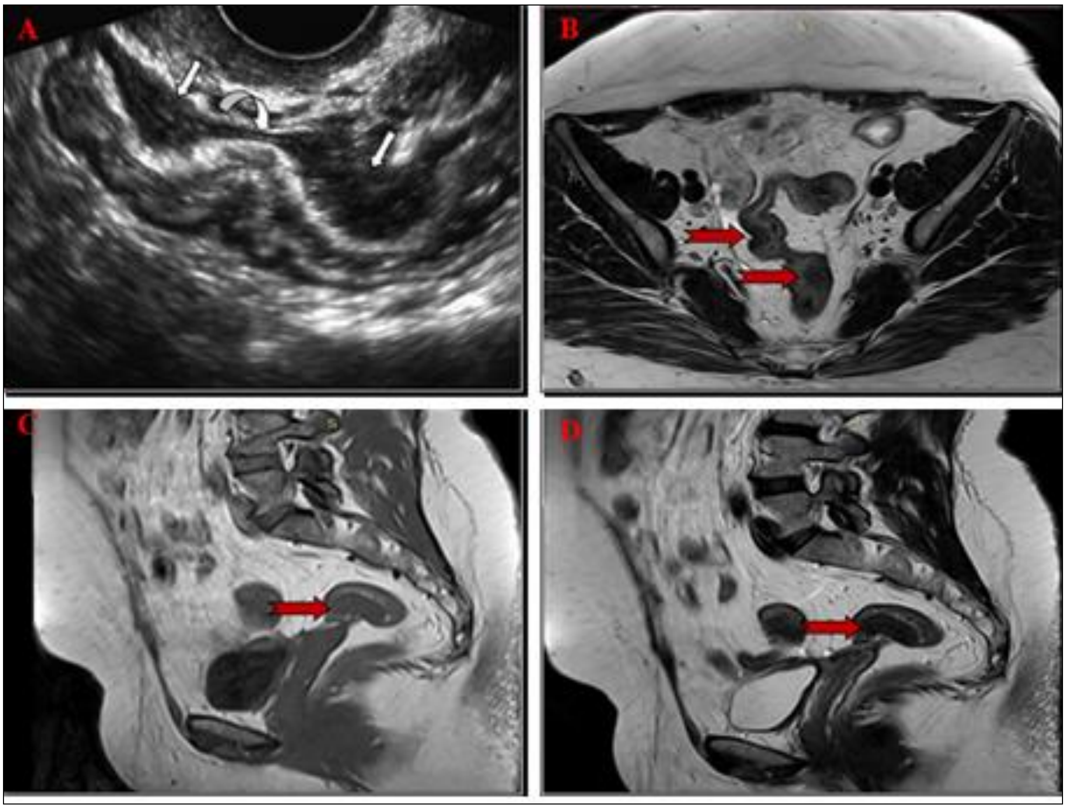

Fig 2: (A) Ultrasound: showed well defined hypoechoic mural nodules seen in rectum & sigmoid colon. (B) MRI axial T_2, (C) MRI sagittal T_1 and (D) MRI sagittal T_2 revealed: multiple nodules in rectosigmoid and anterior rectal wall displaying iso signal intensity in T_1 and low signal intensity in T_2

Case (3): A 35-year-old woman presents with recurrent episodes of left lower abdominal discomfort and oedema.

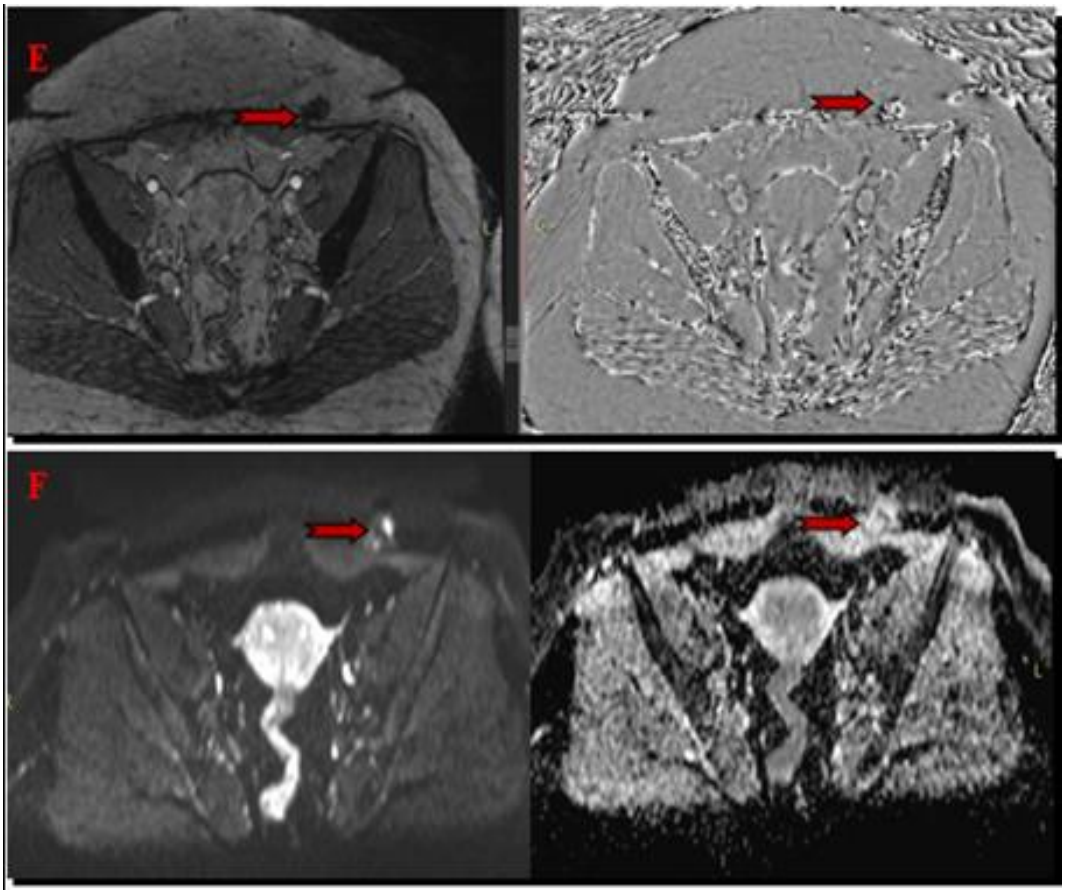

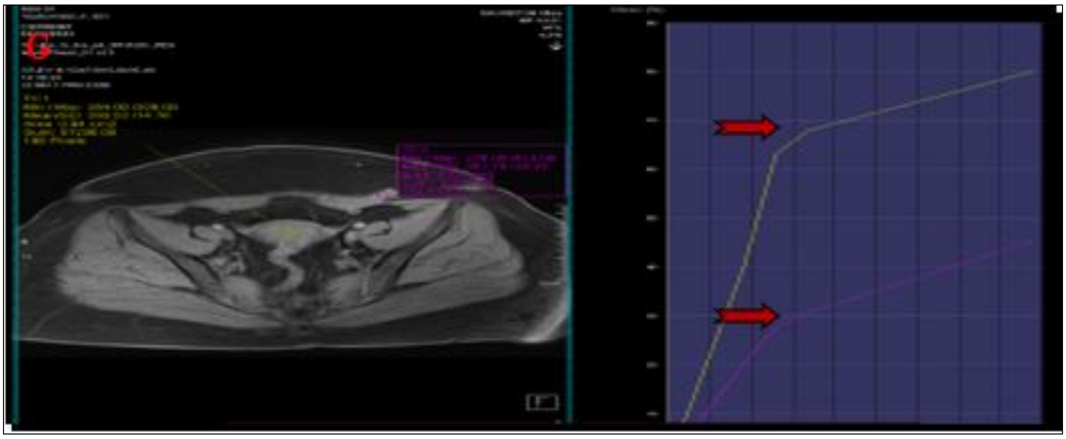

Fig 3: (E) MRI axial SWAN & FILTER sequences: foci of signal void (blooming artifact dark signal) in SWAN sequence with opposing dark signal in FILTER sequence (left-handed apparatus). (E) MRI axial DWI with *b*=8000 sec/mm^2 revealed: focal restricted diffusion (bright signal) & ADC value was 0.94 x 10^{-3}mm^2/sec. (f) DCE MRI show moderate contrast enhancement with curve parrelel to endometrial curve (type 1 curve shows gradule progressive enhancement pattern)

Statistical analysis

Data were entered into the computer and analysed using the IBM SPSS software programme version 20.0. (Armonk, NY: IBM Corp) The qualitative data were described using numbers and percentages. The Kolmogorov-Smirnov test was employed to confirm the normality of the distribution. Quantitative data were reported using range (minimum and maximum), mean, standard deviation, and median. Chi-square test: Used to compare distinct groupings of category variables. Fisher's Exact or Monte Carlo adjustment: Chi-square correction when more than 20% of the cells have an anticipated count of less than 5. Student t-test: Used to compare two groups of normally distributed quantitative variables. F-test (ANOVA): For normally distributed quantitative variables comparing more than two groups, and Post Hoc test (Tukey) for pairwise comparisons. Mann Whitney test: For comparing two groups with improperly distributed quantitative variables. Kruskal-Wallis test: For comparing more than two examined groups with abnormally distributed quantitative variables, and Post Hoc (Dunn's multiple comparisons test) for pairwise comparisons. Kappa (): The Kappa test for agreement was applied. Receiver operating characteristic curve (ROC): The ROC curve provides for a comparison of performance between two experiments. The significance of the acquired findings was assessed at the 5% level.

Results

Their age ranged from 20-45 years with a mean of age was 31.667±6.825 years. The most prevalent age range was 25-35 years, with 18 cases comprising 60% of the total. Most of the patients investigated (86.7 percent) complained of pelvic discomfort and infertility (50).

Table 1: Showing age distribution of patients in this study group and Identification endometriosis in positive cases:

Age groups		
	N	%
< 25 Years	5	16.67
25-35 Years	18	60.00
>35 Years	7	23.33
Range	20-45	
Mean ±SD	31.667±6.825	
Median (IQR)	31.50(27-35)	

Table 2: Showing clinical presentation in this study group and Identification endometriosis in positive cases:

Complaint	Number of cases	Percentage
Pelvic pain	26	86.7%
Menorrhgia	14	46.7%
Infertility	15	50%
Dysmenorrhea	22	73.3%
Dysparunia	14	46.7%
Cyclic painful swelling	3	10%

We calculate ADC value of all endometriotic lesions and adenomyosis to be 1.01, this is the mean value, with 0.468 standard deviation. Surgery and Histopathological examination are the only confirmatory methods for the lesion. Table (3)

Table 3: Mean ADC value in studied cases and Distribution of the studied cases according to US, MRI and laparoscopic results (n = 30):

ADC value	
Range	0.25-2.1
Mean ±SD	1.011±0.468
Median (IQR)	0.995(0.69-1.25)

Laparoscopy revealed 27 positive cases. MRI with DWI, SWI, and DCE combined revealed 26 true positive instances. 1 tubal endometriosis, 2 CS endometriosis, 4 deep infiltrating endometriosis, 10 adenomyosis, and 9 ovarian endometrioma were diagnosed as positive cases as showed in table (4).

Table 4: Data of positive cases and negative cases

	Negative		Positive	
	N	%	N	%
US	7	23.33	23	76.67
Conventional MRI	6	20.00	24	80.00
Functional MRI	4	13.33	26	86.67
Laparoscopic results	3	10.00	27	90.00

We conducted a comparison of the diagnostic performance of the US, conventional MRI, and functional MRI (DWI, SWI, and Dynamic contrast enhanced MRI) in surgically proved instances, as shown in the table below

Table 5: Distribution of studied cases according to different parameters

		Laparoscopic results						Chi-Square		Sensitivity	Specificity	PPV	NPV	Accuracy
		Negative		Positive		Total								
		N	%	N	%	N	%	X2	P-value					
US	Negative	1	33.33	6	22.22	7	23.33	0.186	0.666	77.78	33.33	91.30	14.29	73.33
	Positive	2	66.67	21	77.78	23	76.67							
Conventional MRI	Negative	1	33.33	5	18.52	6	20.00	0.370	0.543	81.48	33.33	91.67	16.67	76.67
	Positive	2	66.67	22	81.48	24	80.00							
Functional MRI	Negative	3	100.00	1	3.70	4	13.33	21.667	<0.001*	96.30	100.00	100.00	75.00	96.67
	Positive	0	0.00	26	96.30	26	86.67							

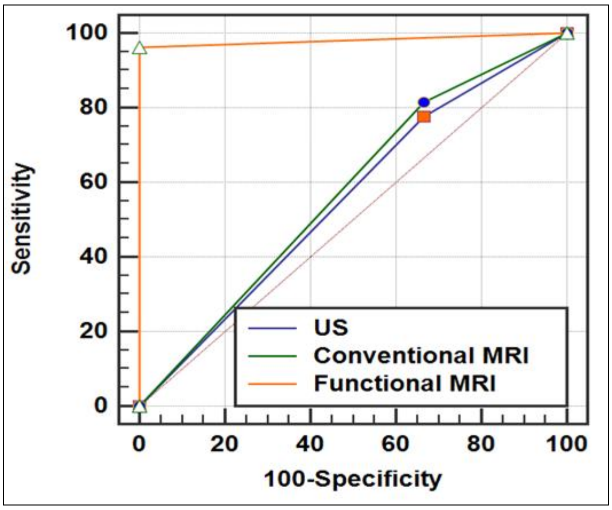

Fig 4: Show the sensitivity and 100 specificity

Discussion

MR imaging is the method of choice for endometriosis staging due to its higher soft tissue contrast. A variety of functional MR imaging approaches, including diffusion-weighted (DW-) MR imaging, dynamic contrast enhanced (DCE-) MR imaging, and susceptibility (SWI), have recently been used to increase imaging information [8].

The primary goal of this research was to assess the functional magnetic resonance appearance of various symptoms of pelvic endometriosis.

In our analysis, uterine adenomyosis was the most common, accounting for 11 cases (36.7 percent), followed by ovarian endometrioma (10 cases (33.3 percent), deep infiltrating endometriosis (DIE) (5 cases (16.7 percent), cs endometrioma (3 cases (10 percent), and tubal endometriosis (1 case) (1.03 percent). This is similar to the research of Benagiano *et al* (2009) [9]. The primary goal of this research was to assess the functional magnetic resonance appearance of various symptoms of pelvic endometriosis.

Our study found that uterine adenomyosis accounted for 36.7% of all cases, followed by ovarian endometrioma (33.3%), cs endometrioma (10.3%), deep infiltrating endometriosis (16.7%), and tubal endometriosis (1.0%). (1.03 percent) The findings here are consistent with those of Benagiano *et al*. (2009) [9].

11 cases (36.7% of total) were diagnosed with uterine adenomyosis, followed by 10 cases (33.3%) of ovarian endometrioma, 5 cases (16.7%) of deep infiltrated endometriosis (DIE), 3 instances (10%) of cs endometrioma, and 1 case (10%) of tubal endometriosis (1.03 percent) Consistent with the findings of Benagiano *et al*. (2009) [9].

The results of this research contradict those of a prior one by Bazot *et al*. (2004) [10] where preoperative MRI showed adenomyosis in only 27% of patients with pelvic endometriosis. Endometriosis, he discovered, most often manifests itself in the pelvic peritoneum and ovaries. Surgery verified pelvic endometriosis in 163 (83.6%) of 195 patients, with histologic evidence of the disease present in at least one pelvic organ (ovary, peritoneum, subperitoneal region). Endometriomas (111; 68.1%), superficial peritoneal implants (83; 50.9%), and deep pelvic endometriosis (103; 63.2%) were identified at surgery alone or at surgery plus biopsy in 163 patients with confirmed pelvic endometriosis [10].

Based on their symptoms and the results of a transvaginal ultrasound (TVUS), 11 patients in our research were diagnosed with adenomyosis, and conventional MRI revealed the characteristic signal in 9 of them, with hyperintense foci on T1 WI and low signal with hyperintense foci (Cysts) on T2WI. This agrees with the results reported by Graziano *et al*. (2015) [11]. In one instance, a diagnosis of fiberoid was initially made using conventional MRI techniques, but the use of DWI revealed intermediate signal (partially restricted with high ADC (1.03x103 mm2/s), and SWI revealed foci of+ signal voids denoting hemorrhagic character, leading to a diagnosis of focal adenomyosis via functional MRI, which was later confirmed surgically via laparoscopy. One possible instance of localised adenomyosis was identified.

The absence of signal gaps on SWI confirmed the proper diagnosis of fibroid. Adenomyosis is better diagnosed with DWI and SWI on an MRI.

Takeuchi *et al*., 2009 [12] tiny haemorrhagic foci in adenomyosis may be seen on susceptibility-weighted imaging as patchy signal voids; this can aid in distinguishing adenomyosis from focal contraction. SWI reveals signal gaps at certain locations, which stand for ectopic endometrium's cyclic hge. This in line with a study done by Takeuchi *et al*., 2019 [13] who found that susceptibility-weighted MRI is sensitive to hemosiderin deposition, showing signal voids within adenomyosis, red degeneration of uterine leiomyoma, and hemorrhagic infarction due to venous blockages.

Ten patients were sent to the MRI unit in our research after the clinical presentation and sonography suggested that they had endometriotic cysts.

This agreed with Takeuchi *et al*., 2019 [13], who claimed that endometrioma diagnosis accuracy might be enhanced by adding SWI, which is sensitive to bleeding in various stages, to conventional MRI. Pathologic features of endometrioma include the deposition of hemosiderin-laden macrophages along the cyst wall, which is caused by the endometrial glands and stroma that are responsible for the cyclic bleeding. Dots and curved signal voids within the cyst and along its wall were clearly seen in our research.

According to research by Pin *et al*., (2019) [14] all lesions

showing up as numerous signal voids on SWI are indicative of haemorrhage [14] who indicated that about 81% of the endometriosis lesions had signal losses on the SWAN sequence related to haemorrhagic character whereas only 52% of the lesions had T1-weighted hyperintense implants. Using the SWAN sequence resulted in better diagnostic performance of the MRI exam than the standard MR protocol (Se = 94% and Spe = 73% in full protocol and Se = 88% and Spe = 69% in conventional MR protocol) [14].
Our present study was a prospective investigation of the use of MR imaging for radiological endometriosis diagnosis. MRI was shown to have a sensitivity of 96.6%, a specificity of 96.6%, and an accuracy of 93.6%. Our findings are consistent with those of Raafat *et al*., (2021) [4], who found that signal voids were seen in 50 of 52 endometriomas and adenomyosis when T_2*WI was also used. Therefore, the sensitivity increased from 65.4% using traditional imaging to 96.15% using T_2*. The inclusion of T_2* increased specificity from 71.4% by using traditional imaging to 85.7%.

Our study has several limitations
Possibly skewed results due to a small sample size, Besides apparent MR contraindications like cardiac pacemakers, decreased state of awareness, vomiting, agitation, and hemodynamic compromise are the primary causes leading to exclusion from MRI. Renal insufficiency is a contraindication to contrast-enhanced MRI. Our investigation was limited by the fact that only two lesions were classified as non-endometrial hemorrhagic cysts, and it is possible that these cysts include hemosiderin-laden macrophages that produce signal gaps on SWI. To confirm the specificity of signal voids along the endometrioma wall on SWI, further examples of hemorrhagic cysts are needed. Signal voids generated by blood-products, particularly in tiny and deep endometriosis foci, may be difficult to detect due to susceptibility artefacts caused by intestinal gas. Due to the rarity of these injuries, the evaluation of the anterior and lateral compartments fell short.

Conclusions
Since DWI and SWI can identify the hemorrhagic nature of endometriotic lesions, they may be used in lieu of invasive laparoscopy to make a diagnosis of endometriosis, which greatly improves the diagnostic accuracy of MRI. In order to confirm that they may substitute for invasive laparoscopy in the diagnosis of endometriosis, larger-scale studies are required.
DCE MRI is also quite helpful in assessing endometriotic lesions that have undergone malignant transformation or those with unusual cytology.

Financial support and sponsorship: Nil.

Conflict of Interest: Nil.

References
1. Bazot M, Bharwani N, Huchon C, Kinkel K, Cunha TM, Guerra A, *et al*. European society of urogenital radiology (ESUR) guidelines: MR imaging of pelvic endometriosis. Eur Radiol. 2017;27:2765-75.
2. Jha P, Sakala M, Chamie LP, Feldman M, Hindman N, Huang C, *et al*. Endometriosis MRI lexicon: Consensus statement from the society of abdominal radiology endometriosis disease-focused panel. Abdom Radiol (NY). 2020;45:1552-68.
3. 3 Fraser MA, Agarwal S, Chen I, Singh SS. Routine vs. expert-guided transvaginal ultrasound in the diagnosis of endometriosis: a retrospective review. Abdom Imaging. 2015;40:587-94.
4. Raafat M, Talaat SH, Abdelghaffar SM, Ali EA. Can diffusion and T_2 star-weighted magnetic resonance imaging aid in the diagnosis of ectopic endometrium? Egyptian Journal of Radiology and Nuclear Medicine. 2021;52:137.
5. Haacke EM, Xu Y, Cheng YC, Reichenbach JR. Susceptibility weighted imaging (SWI). Magn Reson Med. 2004;52:612-8.
6. 6 Koyama T, Togashi K. Functional MR imaging of the female pelvis. J Magn Reson Imaging. 2007;25:1101-12.
7. Tanaka YO, Yoshizako T, Nishida M, Yamaguchi M, Sugimura K, Itai Y. Ovarian carcinoma in patients with endometriosis: MR imaging findings. AJR Am J Roentgenol. 2000;175:1423-30.
8. deSouza NM, Rockall A, Freeman S. Functional MR Imaging in Gynecologic Cancer. Magn Reson Imaging Clin N Am. 2016;24:205-22.
9. Benagiano G, Brosens I, Carrara S. Adenomyosis: new knowledge is generating new treatment strategies. Womens Health (Lond). 2009;5:297-311.
10. Bazot M, Darai E, Hourani R, Thomassin I, Cortez A, Uzan S, *et al*. Deep pelvic endometriosis: MR imaging for diagnosis and prediction of extension of disease. Radiology. 2004;232:379-89.
11. Graziano A, Lo Monte G, Piva I, Caserta D, Karner M, Engl B, *et al*. Diagnostic findings in adenomyosis: a pictorial review on the major concerns. Eur Rev Med Pharmacol Sci. 2015;19:1146-54.
12. Takeuchi M, Matsuzaki K, Nishitani H. Hyperintense uterine myometrial masses on T2-weighted magnetic resonance imaging: differentiation with diffusion-weighted magnetic resonance imaging. J Comput Assist Tomogr. 2009;33:834-7.
13. Takeuchi M, Matsuzaki K, Harada M. Clinical utility of susceptibility-weighted MR sequence for the evaluation of uterine sarcomas. Clin Imaging. 2019;53:143-50.
14. Pin L, Monseau-Thiburce AC, Ziade-Coularis C, Benjamin A, Menut F, Brun JL, *et al*. Exploratory study of the interest of MR susceptibility-weighted imaging for the pre-operative assessment of pelvic endometriosis extent. Eur J Radiol. 2019;118:245-50.

How to Cite This Article
El Dine NMS, Dawoud MM, Abd El-mabod NM, El- Deeb BS. Functional magnetic resonance imaging (MRI) in diagnosis of pelvic endometriosis. International Journal of Radiology and Diagnostic Imaging 2024; 7(1): 01-07.